

# Launch and Deployment Analysis for a Small, Medium Earth Orbit, Technology-Demonstration Satellite

Stephen A. Whitmore\* and Tyson K. Smith†  
*Utah State University, Logan, Utah 84322-4130*

DOI: 10.2514/1.39832

A trade study investigating the economics, mass budget, and concept of operations for delivery of a small technology-demonstration satellite to a medium-altitude Earth orbit is presented. The mission requires payload deployment at a 19,000-km orbit altitude and an inclination of 55 deg. Because the payload is a technology demonstrator and not part of an operational mission, launch and deployment costs are a paramount consideration. The payload includes classified technologies; consequently a U.S.A. licensed launch system is mandated. A preliminary trade analysis is performed where all available options for Federal Aviation Administration licensed U.S. launch systems are considered. The preliminary trade study selects the Orbital Sciences Minotaur V launch vehicle, derived from the decommissioned Peacekeeper missile system, as the most favorable option for payload delivery. To meet mission objectives, the Minotaur V configuration is modified, replacing the baseline fifth stage ATK-37FM motor with the significantly smaller ATK Star 27. The proposed design change enables payload delivery to the required orbit without using a sixth stage kick motor. End-to-end mass budgets are calculated, and a concept of operations is presented. Monte Carlo simulations are used to characterize the expected accuracy of the final orbit. An optimal launch trajectory is presented.

## Nomenclature

$a$	= semimajor axis of orbit, km
$C3$	= specific launch energy, $\text{km}^2/\text{s}^2$
$E$	= separation spring stored potential energy, J
$e$	= orbit eccentricity
$I_{\text{sp}}$	= specific impulse, s
$i$	= orbit inclination, deg
$j$	= iteration index
$n$	= pitch-profile decay exponent, $1/\text{s}^n$
$R_a$	= apogee radius, km
$R_p$	= perigee radius, km
$R_{\text{target}}$	= target apogee radius, km
$t$	= time from launch, s
$V_r$	= local inertial vertical velocity, km/s
$V_v$	= local inertial horizontal velocity, km/s
$\gamma$	= inertial flight path angle, deg
$\Delta V$	= required velocity change during orbit insertion, km/s
$\theta(t)$	= optimal pitch angle profile time history, deg
$\theta(t)_{\text{ballistic}}$	= ballistic angle profile time history, deg
$\lambda$	= pitch-profile decay slope parameter, $1/\text{s}^n$
$\Omega$	= right ascension of ascending node, deg
$\omega$	= argument of perigee, deg

## I. Introduction

SANDIA National Laboratory is investigating advanced technologies required for nuclear explosion monitoring sensors to be deployed with the next generation of Global Positioning

Presented as Paper 1131 at the 46th AIAA Aerospace Sciences Meeting and Exhibit, Reno, NV, 7–10 January 2002; received 16 July 2008; accepted for publication 15 September 2008. Copyright © 2008 by Utah State University. Published by the American Institute of Aeronautics and Astronautics, Inc., with permission. Copies of this paper may be made for personal or internal use, on condition that the copier pay the \$10.00 per-copy fee to the Copyright Clearance Center, Inc., 222 Rosewood Drive, Danvers, MA 01923; include the code 0022-4650/09 \$10.00 in correspondence with the CCC.

\*Assistant Professor, Mechanical and Aerospace Engineering Department, 4130 Old Main Hill/University Mail Code 4130. Associate Fellow AIAA.

†Graduate Research Assistant, Mechanical and Aerospace Engineering Department, 4130 Old Main Hill/University Mail Code 4130. Student Member AIAA.

System (GPS III) satellites. The next generation GPS III constellation architecture will exploit new sensor and signal processing technologies. These emerging technologies must be developed, matured, and space qualified before deployment with the operational constellation. To meet this need, Sandia has proposed a small, free-flying, satellite with a prototype bus architecture. The mission will deploy in a medium Earth orbit (MEO) and have a 1- to 3-year duration. The program has been dubbed “SandiaSat.” The Utah State University (USU) Space Dynamics Laboratory and several of the academic departments within the College of Engineering at USU are assisting Sandia in developing a notional mission plan, together with concept of operations (CONOPS), preliminary satellite and ground station designs, launch options, and associated cost, schedule, and other programmatic estimates. This paper will address the available launch and deployment options.

Fundamental mission objectives require the payload to be delivered to a circular orbit at 19,000 km altitude at an inclination of 55 deg. At this altitude, the ascending node precesses at approximately 10 deg/day; however, the orbit right ascension, argument of perigee, and true anomaly (phasing within the orbit) are not critical to the mission. The deployment orbit was selected to be a “junk orbit” and postmission deorbit of both the payload and expended apogee kick stage is not required. Table 1 summarizes the primary orbit requirements for the MEO mission. It is anticipated that the completed SandiaSat system will be available for launch during the first quarter of calendar year 2012.

## II. Launch Vehicle Selection

Because the orbit requirements are very general, a wide array of launch options is available for payload delivery. Many factors drive the selection of the best commercial launch systems. Key in this analysis phase is the selections of a launch system with adequate performance to deliver the payload mass to the required orbit while allowing for sufficient mass margin. The MEO orbit selected for this study is considerably higher than the nominal orbits considered for small launch systems. Typically, for these high altitude orbits, larger medium-lift launch vehicles are the system of choice. However, the small estimated mass of this payload (<350 kg) allowed the consideration of small launchers originally intended for low Earth orbit (LEO) delivery. For the SandiaSat mission there are three primary constraints on the launch system selection: 1) cost, 2) security, and 3) launch availability. Because the payload is part of

**Table 1 Required orbit parameters**

Parameter	Requirement (accuracy)	Verification method	Design compliance
Orbit altitude	The nominal orbit altitude shall be $\sim 19,000$ km ( $\pm 25$ km)	Verification by launch vendor	Expected compliant based on Monte Carlo simulations
Orbit inclination	The nominal orbit inclination shall be 55 deg ( $\pm 0.25$ deg)	Verification by launch vendor	Expected compliant based on Monte Carlo simulations

a technology-demonstration program and not an operational mission, launch and delivery costs are a paramount consideration. The payload includes classified technologies and the use of a USA licensed launch system is mandated. Finally, the high inclination (55 deg) orbit required for this mission favors a launch from the NASA Wallops Flight Facility (WFF). Several launchers can reach this orbit from the Cape Canaveral Air Force Base (CCAFB) test range, but these require a significant inclination change during launch. This plane change results in a decrease in available payload. Additionally, the availability of launch windows for small payloads from WFF is significantly higher than CCAFB, and the cost of launch operations is significantly lower. Chiulli [1] presents detailed launch site information.

A preliminary trade analysis was performed to consider every available U.S. launch system. The preliminary trade relied on manufacturers' mission payload charts as well as impulsive  $\Delta V$  and rocket equation calculations performed using data derived independently from the manufacturers' published system information. Sellers [2] discusses the details of and procedures for these calculations. Systems with launches available from WFF were given priority in the trade analysis. Launches from the west coast test range at Vandenberg Air Force Base are incompatible with the required orbit inclinations and were not considered for this mission.

#### A. Preliminary Launch Systems Trade Analysis

Currently, there are nine Federal Aviation Administration certified launch systems licensed to carry a classified USA payload. Isakowitz et al. [3] present detailed information of all currently operational or proposed future launch systems. Each of these launch systems were considered for this preliminary analysis. These launch systems are as follows (vendors in parentheses):

1) Atlas (United Launch Alliance) (Atlas, *Encyclopedia Astronautica*, <http://www.astronautix.com/lvs/atlas.htm> [retrieved 1 December 2007]).

2) Athena (Lockheed Martin Aerospace) (Athena 1, *Encyclopedia Astronautica*, <http://www.astronautix.com/lvs/athena.htm> [retrieved 1 December 2007]; Athena 2, *Encyclopedia Astronautica*, <http://www.astronautix.com/lvs/athena2.htm> [retrieved 1 December 2007]).

3) Delta (United Launch Alliance) (Delta, *Encyclopedia Astronautica*, <http://www.astronautix.com/lvs/delta.htm> [retrieved 1 December 2007]).

4) Pegasus (Orbital Sciences Corporation) (Pegasus Users Guide, Orbital Sciences Corporation, Release 6.0, August 2007, <http://www.orbital.com/NewsInfo/Publications/peg-user-guide.pdf> [retrieved 11 May 2008]).

5) Taurus (Orbital Sciences Corporation) (Taurus Launch System Payload User's Guide, Release 4.0, Orbital Sciences Incorporated, March 2006, <http://www.orbital.com/NewsInfo/Publications/taurus-user-guide.pdf> [retrieved 15 May 2007]).

6) Minotaur (Orbital Sciences Corporation) (Minotaur V Fact Sheet, Orbital Sciences Incorporated, [http://www.orbital.com/NewsInfo/Publications/Minotaur\\_V\\_fact.pdf](http://www.orbital.com/NewsInfo/Publications/Minotaur_V_fact.pdf) [retrieved 2 December 2007]).

7) Falcon (Space-X) (Falcon 1 Overview, Space Exploration Technologies, <http://www.spacex.com/falcon1.php> [retrieved 2 December 2007]; Falcon 9 Overview, Space Exploration Technologies, <http://www.spacex.com/falcon9.php> [retrieved 2 December 2007]).

8) Space Shuttle (United Space Alliance, NASA) (Space Shuttle, *Encyclopedia Astronautica*, <http://www.astronautix.com/craft/spauttle.htm> [retrieved 2 December 2007]).

9) Zenit3SL (Sea Launch Odyssey LTD, Multi-National) (Zenit 3SL, *Encyclopedia Astronautica*, <http://www.astronautix.com/lvs/zenit.htm> [retrieved 2 December 2007]).

All of the members of the Atlas family along with the Delta III, Delta IV, and Zenit launch systems have medium- or heavy-lift geostationary transfer orbit (GTO) capability and were primarily designed for large military payloads or for sizable geostationary communications satellite. They all possess "excess lift" capability and have launch costs that vary from \$75 million–\$170 million. For this small technology-demonstration program the costs of these systems were considered to be prohibitive. During the late 1990s, riding along with the space shuttle as a secondary payload on one of the International Space Station (ISS) supply missions would have been an attractive option. But with the impending retirement of the space shuttle in 2010, the shuttle was eliminated from consideration for this mission. The Athena I, Falcon 1, Minotaur I, and Pegasus XL launchers have insufficient lift capability and were eliminated from consideration. The larger Space-X Falcon 9 medium-lift launch vehicle is not considered to be of sufficient maturity to be recognized during this trade analysis.

The Athena II and Delta II launch systems have sufficient lift capacity for the MEO mission and have moderate costs varying from \$22 million (Athena II) to \$60 million (Delta II). The main concern with the Delta II launch system is the availability after 2010 (Delta II's Fate Worries Nonmilitary Users, *Wall Street Journal On-line*, [http://online.wsj.com/article/SB118039764439516631.html?mod=googlenews\\_wsj](http://online.wsj.com/article/SB118039764439516631.html?mod=googlenews_wsj), 29 May 2007 [retrieved 3 December 2007]). This uncertainty of availability makes the Delta II a high programmatic-risk option and for this single reason the Delta II will not be considered further in this trade analysis. The Orbital Sciences Corporation (OSC) Taurus XL, Minotaur IV, and Minotaur V launch systems all have GTO capability with costs varying from \$18 million (Taurus) to \$28 million (Minotaur V). (Verbal quote from OSC, \$35 million first flight, \$25 million–\$28 million recurrent costs thereafter.) These costs are considered to be within the scope of the allowable programmatic costs, and these three OSC systems along with the Athena II were added to the "short list" for further consideration in this trade analysis.

#### B. Secondary Launch Systems Trade Analysis

The preliminary trade analysis presented in the previous section confirmed the generally accepted notion that traditional high-energy launch systems are not economically feasible for the small satellite community. The acceptable short list included only four commercial launch configurations: 1) Lockheed Martin Athena II, 2) OSC Taurus XL, 3) OSC Minotaur IV, and 4) OSC Minotaur V. The comparative positives and negatives of these systems are listed in Table 2. Costs are similar with the Taurus (\$18 million–\$20 million) being the least expensive and the Minotaur V (\$25 million–\$28 million) being the most expensive.

One additional consideration here is the fact that Athena II can only be launched from CCAFB (for easterly launches). Stage impact restrictions limit the maximum CCAFB inclination to 50 deg without a plane change during the stage 3 burn. The required SandiaSat mission inclination of 55 deg mandates a 5-deg plane change during launch. This equivalent  $\Delta V$  loss reduces the payload that can be delivered to the required MEO transfer orbit (MTO) orbit. This equivalent lift loss must be considered in the short list trade analysis.

The lift capability of the four candidate launch systems listed in Table 2 is performed using a C3 launch energy analysis. In this analysis, data for lift masses for LEO, GTO, escape velocity, and any other available orbits are curve fitted, and interpolated to the required

**Table 2 Minotaur IV, Minotaur V, Athena II, and Taurus XL launch system comparisons**

Minotaur IV	Athena II
Maximum LEO payload: >1735 kg, possible GTO capable Successful launches: no manifests to date, uses Legacy Peacekeeper stages, 51 launches Launch site: CCAFB, Wallops (28.5–55 deg inclination), Vandenberg (55–120 deg) Cost: \$25 million Negative factors: no operational record, limited lift capability for high-energy orbits	Maximum LEO payload: 820–2065 kg Successful launches: 6 of 7 since 1995  Launch Site: CCAFB (28.5–50 deg inclination) Kodiak (64–116 deg inclination) Cost: \$22 million–\$26 million Negative factors: inclination restrictions, limited lift capacity, only 590 Kg to GTO
Minotaur V	Taurus XL
Maximum LEO payload: >2500 kg, high-energy version of Minotaur IV Successful launches: no manifests to date, uses Legacy Peacekeeper stages, 51 launches Launch site: CCAFB, Wallops (28.5–55 deg inclination), Vandenberg (55–120 deg) Cost: \$25 million–\$28 million Negative factors: no operational record, development costs for initial flights	Maximum LEO payload: 1590 kg Successful launches: seven of eight since 1995  Launch Sites: CCAFB (28.5–50 deg inclination) Vandenberg (55–120 deg inclination) Cost: \$18 million–\$20 million Negative factors: only 440 kg to GTO

energy level of the MTO orbit. For an elliptical orbit,  $C3$  is a negative value and for an escape trajectory,  $C3$  is nonnegative and equals “excess hyperbolic” velocity. Vallado [4] discusses launch energy concepts in detail.  $C3$  provides a convenient way for comparing the required launch energy orbits with widely disparate orbit parameters. Figure 1 presents curve-fitted  $C3$  data for the Athena II, Taurus XL, Minotaur IV, and Minotaur V launch systems. In these figures the payload mass delivered to a given orbit is plotted against the launch energy. The solid lines represent curve-fit data, and the single data point on each curve represents the payload mass deliverable to the required MTO orbit at 55 deg inclination. The plotted mass does not include the mass of the expended fourth stage. It must also be recognized that these mass estimates are rough and only the comparative launch masses should be considered in this plot.

Lift capacity of the Minotaur V and Athena II far exceed that of the Taurus and Minotaur IV. The Minotaur V provides approximately 8% more lift capacity as well as having the option to launch from Wallops providing for greater launch flexibility. These factors were considered sufficient to weight in favor of the Minotaur V launch vehicle.

### III. Detailed Launch Mission Analysis

This section presents a detailed launch mission analysis based on specifications and properties of the Minotaur V launch vehicle downselected in the previous section. This subsection details 1) the baseline Minotaur V configuration, 2) recommendations for modifications to the baseline, 3) trajectory modeling and

optimization, 4) mission concept of operations, 5) final mass budget analysis, 6) payload separation and recontact analysis, 7) Monte Carlo orbital insertion accuracy analysis, 8) summary of the design options considered, and 9) a rough order-of-magnitude (ROM) cost estimate.

#### A. Baseline Minotaur V Launch System

As described by Schoneman et al. [5], the Minotaur family includes the Minotaur I, IV, and V space launch vehicles and the Minotaur II and III suborbital target launch vehicles. Minotaur vehicles are available from OSC under a contract with the U.S. Air Force (USAF) Space and Missile Systems Center. The Minotaur IV and V systems are constructed using decommissioned government-furnished equipment (GFE) Peacekeeper missile stages (Peacekeeper Missile System, <http://www.techbastard.com/missile/peacekeeper/index.php> [retrieved 15 August 2007]). These GFE stages include stage I (TU-903), stage II (SR119), and stage III (SR120). The Minotaur IV adds a fourth stage based on the Alliant Technology Systems (ATK) launch systems Orion 38 motor. The Minotaur V is a 5-stage evolutionary version of the Minotaur IV, adding propulsive energy needed to support high-energy missions such as GTO or escape velocity. In the Minotaur V configuration the larger ATK launch systems Star 48BV replaces the Orion 38 as the fourth stage motor. The Minotaur V also features an extended payload shroud and

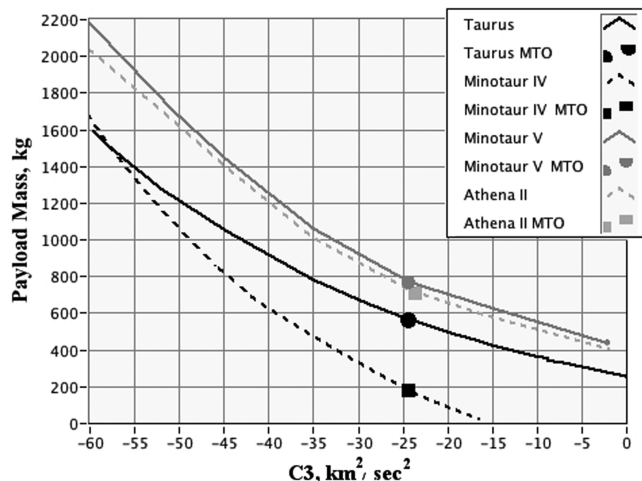


**Fig. 1 Launch energy comparisons for the four candidate launch systems.**

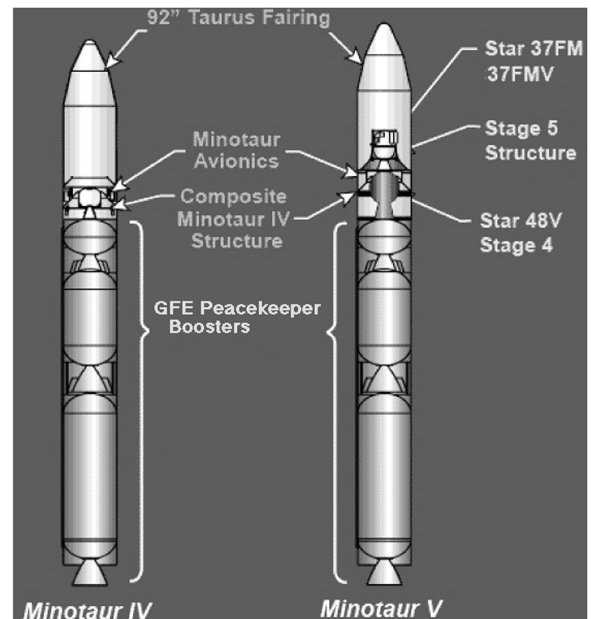


**Fig. 2 Comparison of the baseline Minotaur IV and V launch vehicles.**

support structure for a fifth stage based on the ATK Star 37FM (spin stabilized) or Star 37FMV (3-axis stabilized) kick motor. Figure 2 compares the baseline configurations for the Minotaur IV and Minotaur V launch vehicles (Minotaur Launch System, *Encyclopedia Astronautica*, <http://www.astronautix.com/engines/peapeer1.htm> [retrieved 15 August 2007]).

There have been 13 successful launches from the Minotaur family: seven Minotaur 1 launch vehicles and six Minotaur target vehicles. To date neither the Minotaur IV nor the V systems have been launched. The first scheduled launch of a Minotaur IV in late 2009 will be a USAF payload: the space based space surveillance mission. Even though the Minotaur IV and Minotaur V launch systems have no operational history, collectively, the Peacekeeper stages I–III have successfully launched 51 times with no malfunctions resulting in mission failure. The upper stage ATK Star motors have been flown more than 100 times (ATK Star Motor Overview, Alliant Tech Systems, [http://www.atk.com/customer\\_solutions\\_missionsystems/documents/ATK\\_Catalog\\_May\\_2008.pdf](http://www.atk.com/customer_solutions_missionsystems/documents/ATK_Catalog_May_2008.pdf) [retrieved 6 October 2007]). So there is a proven flight heritage for the majority of the Minotaur IV and Minotaur V subsystems.

### B. Recommended Modifications to the Baseline Minotaur V System

The baseline design for the Minotaur V is intended for high-energy geostationary or escape velocity missions. Typically for these high-energy missions, Minotaur V stages 1–5 are used to insert the payload into the required transfer orbit (e.g., translunar injection), and a sixth stage is integrated with the payload for a final orbit “kick” (e.g., lunar orbit insertion). For the lower energy MEO orbit required for the SandiaSat mission, a sixth stage is unnecessary. This result is somewhat unexpected. Impulsive burn calculations show that the Minotaur V is capable of delivering the required payload to the final MEO orbit in just five stages by replacing the large ATK Star 37 motor with the significantly smaller ATK Star 27 motor. Table 3 compares the Star 37 and Star 27 motors. The STAR 27 rocket motor has a proven flight history and was developed and qualified in 1975 for use as the apogee kick motor for the Canadian Communications Research Center Communications Technology Satellite. The Star 27 motor has served as the apogee kick motor for various applications including the Navigation Satellite Timing and Ranging (NAVSTAR), the Geostationary Operational Environmental Satellite (GOES), and the Geostationary Meteorological Satellite (GMS) series.

The key to achieving the required MEO orbit in five stages is the significantly smaller mass of the Star 27 (360 kg) (Star 27 Motor, ATK Star Motor Overview, Alliant Tech Systems, [http://www.atk.com/customer\\_solutions\\_missionsystems/documents/ATK\\_Catalog\\_May\\_2008.pdf](http://www.atk.com/customer_solutions_missionsystems/documents/ATK_Catalog_May_2008.pdf) [retrieved 6 October 2007]) motor compared to the Star 37 (1148 kg) (Star 37 Motor, ATK Star Motor Overview, Alliant Tech Systems, [http://www.atk.com/customer\\_solutions\\_missionsystems/documents/ATK\\_Catalog\\_May\\_2008.pdf](http://www.atk.com/customer_solutions_missionsystems/documents/ATK_Catalog_May_2008.pdf)

[retrieved 6 October 2007]). Although considerably smaller than the baseline fifth stage motor, the Star 27 actually provides excessive  $\Delta V$  for the final MEO orbit insertion for a 340-kg payload mass. Consequently, a propellant offload will be necessary. The specific offload mass is contingent on the mass of the final delivered payload and the precise transfer orbit used. Fortunately, the Star 27 motor is designed to accommodate various propellant loadings (9% offload previously flown) and can be offloaded up to 20% without recertification. Propellant offloading has the advantage of allowing an option for more payload mass delivery to the required MEO orbit. Using the smaller Star 27 fifth stage motor also allows for significantly more working volume within the Minotaur payload fairing.

### C. Launch Simulation

Because of the proposed modification to the Minotaur V configuration for the SandiaSat mission, and the unusual orbit altitude and inclination, direct simulation of the system components and the trajectory from launch to MEO insertion are necessary to verify the “back of the envelope” calculations presented in the previous section. The direct simulation also offers the opportunity to optimize the mission-specific endo-atmospheric portion of the launch trajectory. The optimization process was facilitated using an interactive simulation developed at Utah State University. This simulation features a graphical user interface that provides for operator interaction and direct in-the-loop control. At each data frame the vehicle pitch angle can be prescribed by direct joystick input, a predefined set of way points, a pitch-profile optimizer, or by a feedback-control loop.

The interactive simulation allows rapid evaluation of a wide variety of candidate trajectories and real-time displays allow users to develop extensive intuition about mission-critical parameters. These “piloted” simulation techniques were pioneered by Evans and Schilling [6] at NASA in the early 1970s during the lifting body flight test programs and are paramount to the analysis presented in this paper. This interactive simulation approach was used as a time-saving measure in lieu of more traditional trajectory optimization tools like the Program to Optimize Simulated Trajectories (POST) developed by Brauer et al. [7]. One of the major drawbacks of POST is the difficulty of setting up the program for Monte Carlo runs and sensitivity of the final solution to the initial trajectory guess. The interactive simulation also allows perturbed conditions about the optimal trajectory for Monte Carlo analysis of expected orbit insertion accuracies. Nonimpulsive, continuous-thrust calculations are used throughout the simulation. Sobol [8] presents a detailed discussion of options and theories for Monte Carlo simulations.

### D. Launch Stage Models

For the first, second, and third stages, engine mass flow, nozzle exit velocity, and nozzle exit pressure are modeled to enable a thrust

**Table 3 Comparison of the ATK Star 37FM and Star 27 motors**

Motor	Star 37 FMV/FM	Star 27
Fully loaded weight	11,483 kg	361.3 kg
Dimensions:		
Length	1.689 m	1.327 m
Maximum width	0.935 m	0.693 m
Manufacturer	ATK/Thiokol	ATK/Thiokol
Case material	Titanium	Titanium
Propellants:		
Mass (fully loaded)	1066.3	333.8 kg
Materials	TP-H-3340 solid	TP-H-3135 solid
Nozzle		
Exit area	0.311 m <sup>2</sup>	0.185 m <sup>2</sup>
Expansion ratio	48.2:1	48.2:1
Pitch, roll, yaw control	3-degrees-of-freedom gimbal FMV fixed nozzle FM, spin stabilized	Fixed nozzle, spin stabilized
Burn time	62.7 s	34.4 s
Thrust	47.3 kN	25.5 kN
$I_{sp}$	289.9 s	287.9 s

**Table 4** Minotaur V stage propulsion properties

Simulation element	Stage 1	Stage 2	Stage 3	Stage 4	Stage 5
Motor	TU-903	SR119	SR120	Star 48V	Star 27
Designer	Thiokol	AEROJET	Hercules	Thiokol	Thiokol
Dry mass, kg	4300	3175.2	635.0	154.6	27.5
Wet mass, kg	48,960.0	27,669.1	7711.1	2164.6	361.3
Thrust (vac), kN	2204.5	1223.3	289.1	68.6	25.4
Thrust (sea level), kN	1954.3	1048.3	235.0	24.2	6.7
Exit area, m <sup>2</sup>	2.469	1.726	0.534	0.439	0.185
Expansion ratio	24.91	41.89	22.50	54.80	48.80
$I_{sp}$ (vac), s	282	309	300	292.1	287.9
Burn time, s	56	60.7	72	85	34.4
Mass flow, kg/s	797.2	403.7	98.28	23.96	9.01
Exit pressure, kPa	47.88	32.26	20.83	10.99	2.79
Exit velocity, m/s	2617.2	2892.3	2828.9	2663.4	2765.9

calculation as a function of altitude. The fourth and fifth stages are modeled using vacuum thrust only. These data were collected from a variety of public domain sources (ATK Launch and Mission Systems, Alliant Tech Systems, [http://www.atk.com/customer\\_solutions\\_missionsystems/documents/ATK\\_Catalog\\_May\\_2008.pdf](http://www.atk.com/customer_solutions_missionsystems/documents/ATK_Catalog_May_2008.pdf) [retrieved 15 August 2007]). An equilibrium gas-chemistry code Chemical Equilibrium with Applications developed by Gordon and McBride [9] was used to model the combustion products based on mean properties for the specified propellants. The combustion data were used to develop the engine models for the first three stages. The aerodynamic characteristics of the first four vehicles stages were estimated using a panel code for subsonic flight conditions (AEROCFD, Apogee Rockets, <http://www.apogeerockets.com> [retrieved 7 October 2007]), and a USU-developed incidence angle code for the supersonic flight conditions (Whitmore, S. A., "Conical Supersonic Flow Fields," Utah State University, [http://www.neng.usu.edu/classes/mae/5420/Compressible\\_fluids/section11.html](http://www.neng.usu.edu/classes/mae/5420/Compressible_fluids/section11.html) [retrieved 15 November 2005]). This code was developed using incidence angle theory as presented by Anderson [10]. As the rocket motors burned, base drag was assumed negligible. During stage separation and the fourth stage coast, plume-off base drag characteristics are calculated using empirical correlations derived from Hoerner [11]. The launch simulation burned each of the four Minotaur stages to exhaustion, assuming a constant engine mass flow, and depleting mass as a function of time. Table 4 presents the engine and stage properties as modeled in the simulation.

#### E. Pitch-Profile Optimization

A pitch-profile optimization is used to deliver the required payload mass to the maximum energy MTO orbit. In this launch profile optimization an "apogee targeting" strategy is used where the fifth stage kick motor and payload are inserted directly into the MTO orbit with fixed (19,000 km) apogee altitude and a variable perigee altitude. The pitch profile is optimized starting with the minimum drag (ballistic) launch profile, and then systematically "turning the corner." The optimal "gravity turn" profile is modeled as an exponential decay from the ballistic pitch profile using a two-parameter model,

$$\theta(t) = \theta(t)_{\text{ballistic}} \cdot e^{-\lambda \cdot t^n} \approx \tan^{-1}(V_r/V_v) \cdot e^{-\lambda \cdot t^n} \quad (1)$$

In Eq. (1),  $\theta(t)$  is the optimal pitch profile,  $\theta(t)_{\text{ballistic}}$  is the ballistic profile,  $\lambda$  is a pitch decay slope parameter,  $n$  is a scaling exponent, and  $t$  is time from launch. The exponential decay produces a smooth turn and assures that angles of attack remain small. This small angle of attack limits aerodynamic side loading on the launch stack and allows the ballistic pitch angle to be approximated by the inertial flight path angle, where  $\gamma = \tan^{-1}(V_r/V_v) \cdot e^{-\lambda \cdot t^n}$ . The local vertical  $V_r$  and horizontal  $V_v$  velocities are consequences of the launch trajectory and are not independent parameters to be optimized.

In the optimization process the parameters  $\{\lambda, n\}$  are set at the beginning of the simulation run and fixed as a function of time. The pitch-profile parameters are iterated between simulation runs to

satisfy the apogee constraint and maximize orbital energy. In the constrained apogee problem, maximizing orbital specific energy is equivalent to maximizing the MTO perigee altitude. Parameter iterations are implemented as two loops with  $n$  being iterated in the outer loop and  $\lambda$  driven to a value that satisfies the apogee constraint in the inner loop. The inner apogee constraint is satisfied using a quasi-Newton–Raphson method

$$\lambda^{(j+1)} = \lambda^{(j)} - \left( \frac{R_a^{(j)} - R_{\text{target}}}{R_a^{(j)}} \right) \lambda^{(j)} \quad (2)$$

where the sensitivity derivative is approximated by  $\partial R/\partial \lambda \approx R_a^{(j)}/\lambda^{(j)}$  to speed convergence time. The parameter pair that gives largest transfer orbit perigee altitude (orbital energy) and satisfies the apogee constraint provides the optimal pitch profile.

This ad hoc optimization method is used in lieu of more traditional Lagrange multiplier methods to save calculations and speed convergence. This constrained optimization insures that the MTO orbit has maximal energy and allows the optimal amount of kick-stage propellant to be offloaded. This offload leaves additional mass available for the SandiaSat payload. Figure 3 shows the optimal pitch model parameters, where panel a) plots the MTO orbital energy versus the exponent parameter ( $n$ ), and panel b) plots the corresponding slope parameter ( $\lambda$ ) that satisfies the orbit apogee constraint. For this delivered mass, the optimal pair is  $\{\lambda = 0.0877 \text{ s}^{-0.54}, n = 0.54\}$ .

#### F. Optimized Simulation Launch Profile

Figure 4 shows an optimized launch profile with a) altitude versus downrange, b) altitude versus time, c) velocity versus time, and d) acceleration versus time being plotted. The initial launch angle is 89.5 deg and the total delivered MTO mass is 1046.4 kg. This delivered mass includes the inert fourth stage and avionics module. Here the first three stages are fired consecutively followed by a Keplerian coast period. The fourth stage motor is fired shortly before the Keplerian orbit apogee to insert the payload into the MTO orbit. Notice that the acceleration plot clearly shows the extended coast time between the third stage motor burnout and the fourth stage motor firing.

As mentioned earlier, the launch pitch profile is optimized to give the maximum MTO orbital energy with a constrained apogee altitude. Figure 5 shows the optimized pitch profile compared against the corresponding ballistic trajectory. Notice that the optimized trajectory initiates the gravity turn far sooner than the ballistic profile and levels out once the endo-atmospheric portion of the flight is completed (approximately 200 s). Different final MTO launch masses and initial launch angles will result in slightly different optimal pitch profiles. The payload shroud is jettisoned midway during the stage 3 burn and is driven by dynamic pressure constraints as prescribed by OSC in the Minotaur launch guide. The resulting optimized transfer orbit has a mean apogee altitude of 19,000 km and a perigee altitude of approximately 1573 km. Also the actual MTO insertion altitude is 1728.6 km, slightly above the orbit perigee.

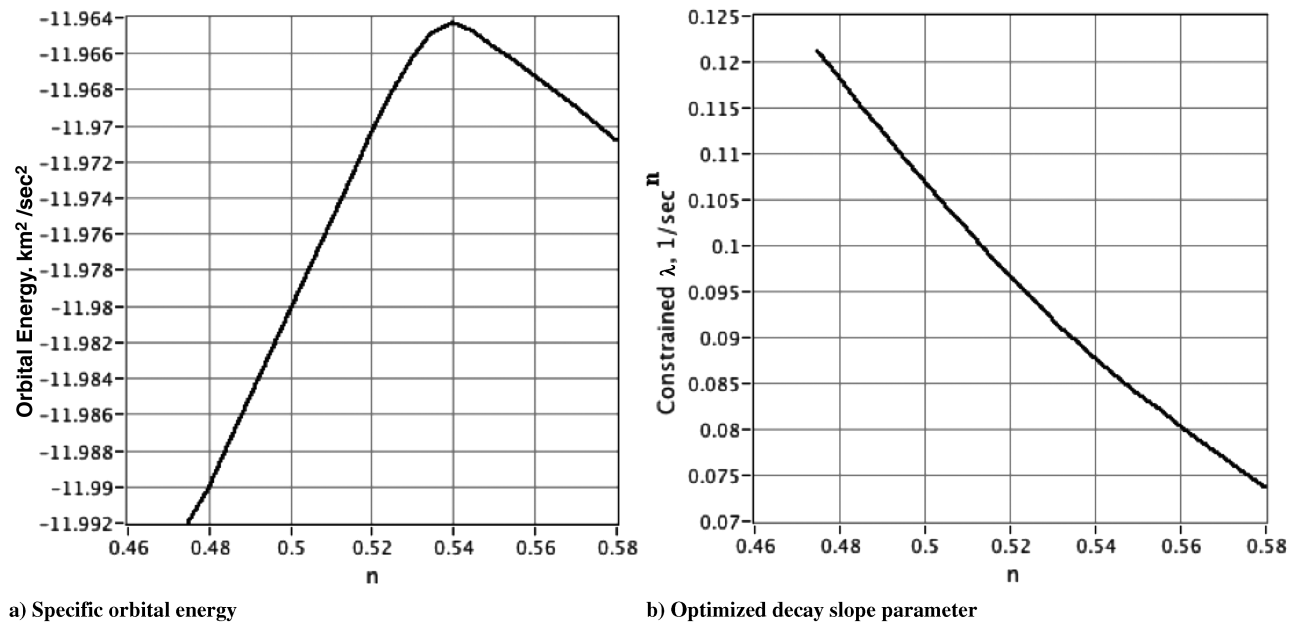


Fig. 3 Optimal pitch model parameters.

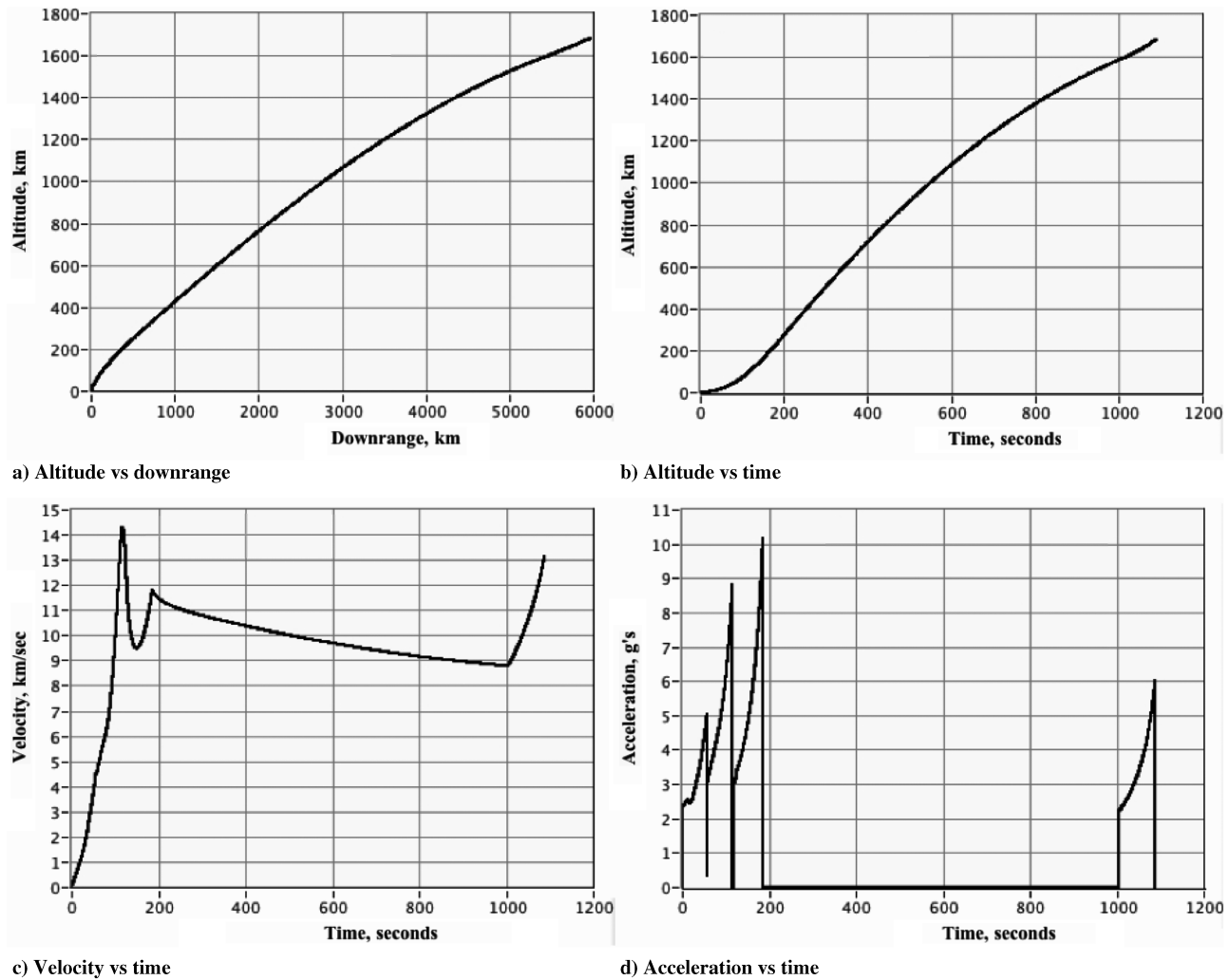


Fig. 4 Optimized Minotaur V MTO launch trajectory.

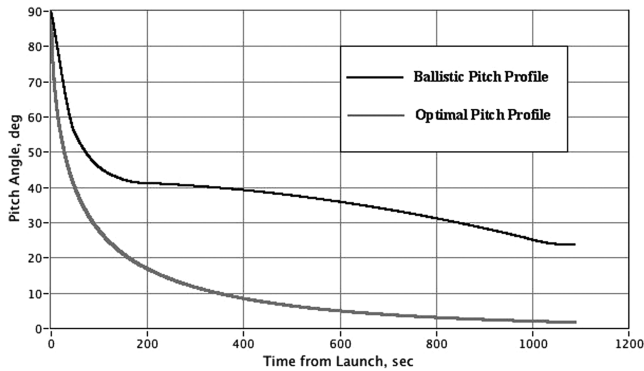


Fig. 5 Optimized launch pitch profile.

### G. Mission Concept of Operations

Figure 6 shows the end-to-end launch and deployment concept of operations (CONOPS). In this CONOPS, the fourth stage (Star 48) inserts the payload and fifth stage (Star 27) into the MTO trajectory. The Minotaur V fourth stage avionics module positions the payload at the required attitude and spins up the system at a rotational rate of approximately 10 rpm. The coast from MTO insertion to the orbit apogee requires approximately 2.8 h. Once MTO apogee is reached, the Star 27 fires and inserts the payload into the circular 19,000 km orbit. Once inserted into the final orbit, a cold-gas jet system attached to the payload adapter cone spins down the payload. Following spin down, the expended fifth stage is separated from the SandiaSat. Total mission elapsed time from launch to solar panel deployment is approximately 3.16 h.

### H. Stage IV, Stage V Mass Budget Analysis

As mentioned in the previous section, the Star 27 kick motor provides excess impulse for the required MTO to MEO orbit transfer. Consequently, the offloading propellant allows more payload to be

Table 5 Stage IV mass budget for optimized launch and MTO insertion

Star 48 motor	Inert motor	154.9 kg
	Full propellant load	2000.8 kg
	Loaded motor mass	2162.9 kg
Stage IV interstage		150.0 kg
Avionics module, spin-up propellant		171.1 kg
Delivered mass to MTO		1046.4 kg
Spacecraft mass after avionics module jettison		725.3 kg

delivered to the final orbit and trajectory optimization balance propellant offload versus the delivered payload mass. The required apogee kick  $\Delta V$  (and hence the propellant offload for the Star 27 fifth stage) depended on the precise MTO trajectory energy level reached during the launch and MTO insertion phase of the mission. Allowing for the mass of the fourth stage avionics module and the inert fourth stage, the “live payload” delivered to MTO apogee is 725.3 kg. Table 5 shows the Stage IV mass budget resulting from the optimized MTO launch analysis.

Based on the 725.3 kg MTO spacecraft mass, Table 6 shows the mass budget for the MEO insertion. Notice that a 26.9% propellant offload is required to “tune” the proper MEO orbit insertion  $\Delta V$ . The delivered 431.6-kg maximum payload offers approximately 22% contingency for growth on the estimated 350-kg nominal SandiaSat mass.

### I. Payload Separation and Recontact Analysis

The separation system chosen for the SandiaSat was the Planetary Systems Corporation 38 in. Motorized Lightband® (Lightband Separation Systems, Planetary Systems Incorporated, <http://www.planetarysystemscorp.com> [retrieved 6 October 2007]). Holemans [12] describe the operational characteristics of this separation system in detail. The Lightband is stowed with links

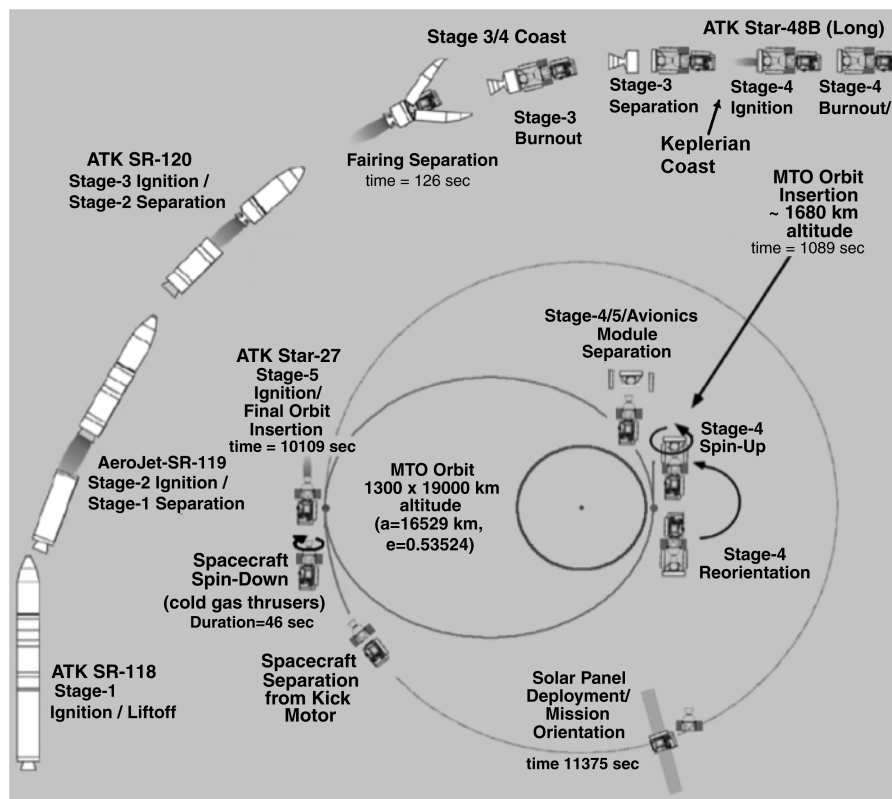
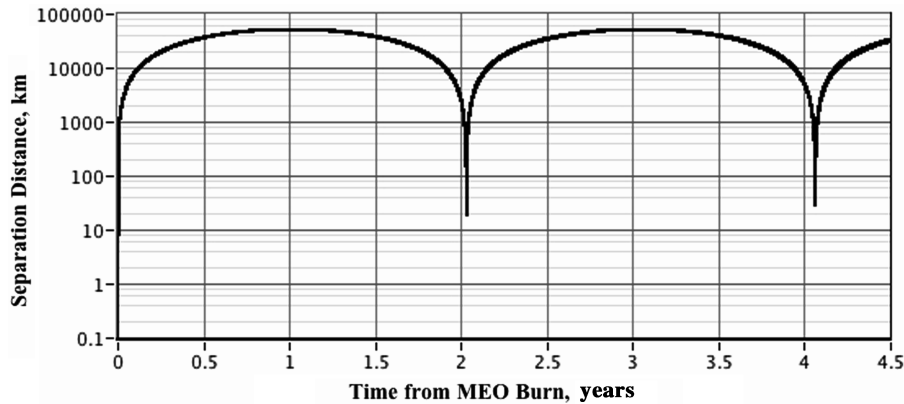


Fig. 6 Launch and deployment concept of operations.

**Table 6 Stage V mass budget for optimized MEO insertion**

Lightband® separation system	Upper ring	2.1 kg
	Lower ring	4.1 kg
Star 27 kick motor	Inert weight	27.5 kg
	Nominal propellant load	333.8 kg
	Actual propellant load	244.0 kg (26.9% offload)
Kick-motor adapter cone		16.0 kg
Delivered mass to MEO		482.0 kg
Spacecraft mass after kick-motor jettison	431.6 kg (excluding mass of separation system upper ring)	

**Fig. 7 Time history of separation distance between payload and expended fifth stage.**

locking a retaining ring that holds the separation system together. Motors drive a mechanism that allows the retaining ring to contract. The contracted ring allows spring plungers to disengage the payload side of the ring, and separation springs push the two rings apart. The separation springs impart  $\Delta V$  to the payload, separating it from the expended fifth stage motor. The resulting separation  $\Delta V$  is determined by the number of separation springs installed in the system (Anon., “2000785 Rev A User’s Manual for Mark II Lightband,” Planetary Systems Incorporated, [http://www.planetarysystems.com/download/2000785A\\_UserManual.pdf](http://www.planetarysystems.com/download/2000785A_UserManual.pdf) [retrieved 05 December 2007]). For this mission 26 separation springs were used and provide a separation force of 2234 N (227.8 kgf). This force can be easily compressed by the weight of the satellite and makes for easier processing during payload installation.

The 26 separation springs provide a separation  $\Delta V$  of 0.83 m/s. Delaying separation for 120 s after Star 27 motor burnout when residual propellant burning is completed, this separation  $\Delta V$  is sufficient to prevent recontact between the payload and exhausted Star 27 casing. Figure 7 shows the results of the separation analysis that assumes  $\Delta V$  is directed with a 5-deg pitch angle and a 5-deg out-of-plane (yaw) angle. The absolute separation distance in kilometers is plotted with a logarithmic scale on the ordinate and the elapsed time from the MEO insertion burn in years is plotted on the abscissa.

Notice that the Lightband system provides immediate and positive separation and a potential recontact event occurs approximately every 2 years. During the maximum lifetime of the mission (3 years) the closest approach between the two objects is 20 km. It is possible that somewhere beyond the lifetime of the SandiaSat satellite the two objects could recontact creating an orbital-debris scenario. But since the SandiaSat MEO orbit is considered a junk orbit this eventuality is not a great concern.

#### J. Monte Carlo Analysis of Expected Orbit Insertion Accuracy

The end-to-end final orbit insertion accuracy is estimated using Monte Carlo analyses where the optimization kernel is run in batch mode with rocket and orbit parameters perturbed using Gaussian-distributed, white noise models. Table 7 shows the 1- $\sigma$  noise inputs to the Monte Carlo model. Model parameters were perturbed for the launch phase, final orbit insertion burn, and payload separation. The Keplerian coast phases of the mission were assumed to be deterministic.

A total of 997 data runs were performed to establish statistical validity [8], and statistics of the final orbital parameters were calculated. Table 8 shows the end-to-end uncertainty estimates in the final MEO parameters. These uncertainties include the effects of the

**Table 7 1- $\sigma$  uncertainty models in end-to-end Monte Carlo simulation**

Launch uncertainties, 1 $\sigma$	Pitch profile, $\pm 0.05\%$ total error (from optimal) Assumes pitch guidance feedback Uncertainty in drag coefficient, $\pm 5\%$ Uncertainty in lift coefficient, $\pm 5\%$ Thrust uncertainty, $\pm 0.1\%$ Burn time uncertainty, $\pm 0.1\%$ Total impulse uncertainty, $\pm 0.1414\%$
Star 27 kick-motor uncertainties, 1 $\sigma$	Thrust error, 0.16667% Burn time uncertainty, 0.084% Total impulse uncertainty, 0.1867% Burn pitch misalignment uncertainty, $\pm 1$ deg Burn out-of-plane misalignment uncertainty, $\pm 1$ deg
Lightband separation uncertainties, 1 $\sigma$	Separation $\Delta V$ uncertainty, $\pm 0.1$ m/s Separation pitch misalignment uncertainty, $\pm 1$ deg Separation out-of-plane misalignment uncertainty, $\pm 1$ deg



**Table 8 End-to-end uncertainty estimates in final MEO orbit parameters**

Parameter	Mean value	1- $\sigma$ standard deviation
$a$ , km	25,370.2	$\pm 80.8$
$e$	0.00124	$\pm 0.0004$
$i$ , deg	54.991	$\pm 0.115$
$\Omega$ , deg	197.71	$\pm 0.080$
$\omega$ , deg	151.25	$\pm 0.119$
Perigee, km	18,975.8	$\pm 83.9$
Apogee, km	19,022.9	$\pm 86.2$

**Table 9 Minotaur V launch ROM cost estimate**

Taurus launch costs	\$20 million
Minotaur V estimate, Taurus + additional nonrecurrent engineering amortized over first 10 flights	\$26 million
Engineering Star 27 interface with fifth stage payload adapter	\$2.5 million
Total ROM	\$28.5 million

**Table 10 Design changes and options considered**

Design baseline change option	Technical performance variation	Programmatic cost variation	Programmatic schedule variation
Minotaur V with Star 37 upper stage	Star 37 too massive for MEO insertion No residual payload		Minimal
Minotaur V with Star 27 upper stage	With $\sim 27\%$ offload, 430 + kg deliverable to MEO	\$250,000 increase	Minimal
26 spring Lightband replaces original 92 spring option	None, allows easier ground handling	Minimal	Minimal, possible time savings

separation  $\Delta V$ . The mean values for the orbit perigee and apogee altitudes derived from the Monte Carlo simulation are compliant with the requirements prescribed in Table 1.

#### K. Rough Order-of-Magnitude Launch Cost Estimate

Because both the Minotaur IV and Minotaur V launch vehicles do not have an operational flight history, any analysis of the launch costs must be regarded as only a ROM estimate. Table 9 summarizes this calculation. The Taurus launch costs are used as the baseline for this calculation [3]. Total recurrent launch costs are estimated at \$28.5 million. OSC estimates the recurrent operational launch costs at \$25 million–\$28 million, so this estimate is consistent with the vendor's claims [5].

### IV. Trade Summary

A trade study investigating the economics, mass budgets, and concept of operation for delivery of a small, technology-demonstration satellite to a medium-altitude Earth orbit is presented. Sandia National Laboratory has proposed this prototype satellite to space test and mature emerging technologies required for the next generation of global positioning satellites. A primary objective is the maturation low readiness technologies required for nuclear explosion monitoring. Mission requirements specify the payload to be delivered to a circular orbit at 19,000 km altitude and an inclination of 55 deg. A preliminary trade analysis is performed where all available U.S. launch systems are considered. The initial trade study identifies the Minotaur V launch system as the best launch option. The Minotaur V is a five-stage evolutionary version of the Minotaur IV constructed using decommissioned government-furnished Peacekeeper missile stages for the first three stages. End-to-end mass budgets are calculated, and a concept of operations is presented. Monte Carlo simulations are used to characterize the expected accuracy of the final orbit. An optimal launch trajectory and an order-of-magnitude cost analysis are presented. Table 10 shows the trade options that were considered and the impacts of these design changes on the program for the MEO launch analysis. The major design consideration was the replacement of the Star 38/FMV fifth stage on the Minotaur V with the smaller Star 27 motor.

### V. Conclusions

A primary conclusion of this study is that replacing the baseline fifth stage ATK-37FM motor by the significantly smaller ATK Star 27 allows the final orbit to be reached without a sixth stage. This unexpected result is very significant in that it offers a less complex

and potentially less expensive launch configuration and provides significantly more working volume within the payload fairing. Other significant conclusions are as follows:

- 1) The optimized trajectory delivers a total of 1046.4 kg to MTO (725 kg minus the inert fourth stage).
- 2) The Star 27 kick motor requires  $\sim 27\%$  offload for proper payload insertion  $\Delta V$ .
- 3) The total spacecraft mass after kick-motor separation is approximately 431.6 kg, a 22% mass margin.
- 4) The Lightband with 26 separation springs provided sufficient  $\Delta V$  to avoid recontact for mission lifetime.
- 5) Monte Carlo analysis shows 1- $\sigma$  apogee/perigee accuracy of approximately  $19,000 \pm 85$  km.
- 6) Monte Carlo analysis shows final orbit inclination of approximately  $55.0 \pm 0.1$  deg.
- 7) The total mission time line from launch to final orbit is approximately 3.16 h.
- 8) Launch costs including amortization of nonrecurrent engineering are estimated at \$28.5 million.

### Acknowledgments

The authors wish to thank Sandia National Laboratories for sponsoring this work and the staff at Space Dynamics Laboratory for their tireless efforts in sorting and editing this material.

### References

- [1] Chiulli, R. M., *International Launch Site Guide*, The Aerospace Press, El Segundo, CA, 1994, Chap. 13.
- [2] Sellers, J. J., *Understanding Space: An Introduction to Astronautics*, 2nd ed., McGraw-Hill, New York, 2000, Chaps. 7, 9.
- [3] Isakowitz, S. J., Hopkins, J. P., Jr., and Hopkins, J. B., *International Reference Guide to Space Launch Systems*, 4th ed., AIAA, Reston, VA, 2003, Chaps. 2, 5, 6, 8, 15, 25, 28, 32.
- [4] Vallado, D. A., *Fundamentals of Astrodynamics and Applications*, 2nd ed., Microcosm Press, El Segundo, CA, 2001, Chaps. 1, 6.
- [5] Schoneman, A., Amorosi, L., Cheke, D., and Chadwick, M., "Minotaur V Space Launch Vehicle for Small, Cost-Effective Moon Exploration Missions," *21st AIAA/USU Conference on Small Satellites*, SSC07-III-2, AIAA, Reston, VA, Aug. 2007.
- [6] Evans, M. B., and Schilling, L. J., "The Role of Simulation in the Development and Flight Test of the HIMAT Vehicle," NASA TM-84912, April 1984.
- [7] Brauer, G. L., Cornick, D. E., and Stevenson, R., "Capabilities and Applications of the Program to Optimize Simulated Trajectories (POST)," *Program Summary Document*, NASA CR-2770, Feb. 1977.

- [8] Sobol, I. M., *A Primer for the Monte Carlo Method*, CRC Press, Boca Raton, FL, 1994, Chaps. 1–3.
- [9] Gordon, S., and McBride, B. J., “Computer Program for Calculation of Complex Chemical Equilibrium Compositions and Applications,” NASA RP-1311, 1994.
- [10] Anderson, J. D., Jr., *Modern Compressible Flow with Historical Perspective*, 3rd ed., McGraw-Hill Higher Education, New York, 2003, Chap. 4.
- [11] Hoerner, S. F., *Fluid Dynamic Drag*, Self-Published Work, Library of Congress Card Number 64-1966, Washington, D.C., 1965, pp. 3-19, 3-20.
- [12] Holemans, W., “The Lightband as Enabling Technology for Responsive Space,” *The Second Annual Responsive Space Conference*, AIAA Paper RS2-2004-7005, April, 2004.

J. Martin  
Associate Editor